

Millimeter-Wavelength Forward-Model Comparisons Based on Ground-Based Radiometric Data Taken During the 1999 NSA/AAO Radiometric Experiment

*E. R. Westwater and M. A. Klein
Cooperative Institute for Research in
Environmental Sciences
University of Colorado*

*National Oceanic and Atmospheric Administration
Environmental Technology Laboratory
Boulder, Colorado*

*P. E. Racette
National Aeronautics and Space Administration
Goddard Space Flight Center
Greenbelt, Maryland*

*D. Cimini
University of L'Aquila
L'Aquila, Italy*

*Y. Han
National Oceanic and Atmospheric Administration
National Environmental Satellite Data and
Information Service
Camp Springs, Maryland*

*A. J. Gasiewski
National Oceanic and Atmospheric Administration
Environmental Technology Laboratory
Boulder, Colorado*

Introduction

Extremely dry conditions commonly occur in high-latitude regions during the winter months. Accurate measurements of the precipitable water vapor (PWV) during such dry conditions are needed to improve our understanding of the regional radiation energy budgets. The strength associated with the 183 GHz water vapor absorption line makes radiometry in this frequency regime promising for measuring low amounts of PWV. However, retrievals using these frequencies are complicated by the uncertainties in absorption models and the fact that radiation at these frequencies also responds to the vertical temperature distribution as well as to the distribution of vapor, liquid, and ice clouds. During March 1999, an experiment was conducted at the Atmospheric Radiation Measurement (ARM) Program's Cloud and Radiation Testbed (CART) site on the North Slope of Alaska/Adjacent Arctic Ocean (NSA/AAO) near Barrow, Alaska, (Racette et al. 2000) to investigate the application of ground-based millimeter wave radiometry for deriving PWV during these dry conditions. Because only a few clear-sky radiosonde measurements were available during the experiment, we also developed a statistical comparison based on the PWV as measured by the ARM microwave radiometer (MWR) (Liljegren 2000) as the dependent variable, and studied the behavior of measured brightness temperature, T_b , as a function of the inferred PWV.

Clear-Sky T_b Measurements

One of the motivating factors in deploying 183 GHz radiometers in the arctic is the limited sensitivity of the 23.8 and 31.4 GHz to low concentrations of vapor and cloud liquid. Conversely, both theoretical and experimental observations have indicated a much greater sensitivity of measurements around the 183 GHz spectral line. This is dramatically illustrated in Figure 1A in which observed T_b s from the ARM MWR, the NASA microwave imaging radiometer (MIR), and the Environmental Technology Laboratory (ETL) circularly scanning radiometer (CSR) during March 1999. For this figure, we show only the MIR and CSR T_b s at 183 ± 7 GHz. Note that the peak-to-peak variation of the MWR is only about 4 K for the entire month, while those of the millimeter wavelength instruments have a range of about 70 K for the same time interval.

Retrieved Precipitable Water Vapor from MWR Measurements

We derived PWV from the ARM MWR using the a priori linear statistical retrieval method applied to one- and two-frequency data vectors of optical depths τ that were derived from the two measured brightness temperatures. A 6-year ensemble of NSA radiosondes was used to derive the retrieval coefficients; a 0.3 K root mean square (rms) radiometric noise level was assumed. The forward model used in the dual-frequency retrievals was from (Rosenkranz 1998), hereafter designated ROS. We also compared single frequency retrievals using ROS and L87 (Liebe and Layton 1987) absorption models: As pointed out previously (Han et al. 2000), there were initial calibration problems with the ARM MWR due to internal temperature control problems, and subsequently the data were recalibrated by the “instantaneous calibration method” of (Han and Westwater 2000). As shown in Figures 1B and 1C, even with this recalibration, there were still calibration inconsistencies of the order of 0.5 K over the entire data period. Two other points are significant: first, the two channel retrievals of L87 and ROS differ only slightly, and also differ only slightly with the single frequency retrieval based on ROS. Because of the 0.5 K difference in the O₂ computation between L87 and ROS, a significant bias difference occurs in the single channel retrievals.

MWR-PWV vs. CSR T_b

As show in the Comparison of T_b from the MWR and MIR with Radiosonde-Based Calculations section of this paper, we compare measured T_b s with calculations based on radiosondes using L87, L93 (Liebe et al. 1993), and ROS absorption models. Here, as a complementary approach that relied on the PWV derived from the ARM MWR, we compared measured T_b s from the CSR vs. PWV derived from the ROS model. We show in Figure 2, comparisons at the 183 +/- 12, +/- 7, and +/- 5 GHz channels. The measured data are 10-min averages. The colored lines were calculated by

$$T_b = T_c \exp(-\tau) + T_{mr} (1 - \exp(-\tau)) \quad (1)$$

and

$$\tau = \tau_d + \kappa \text{PWV}, \quad (2)$$

where T_c is 2.75 K, T_{mr} is the mean radiating temperature, τ_d is the dry optical depth, and κ is the mass absorption coefficient from water vapor. The colored lines were calculated by averaging radiative transfer calculations (T_{mr} , τ_d , κ) based on radiosondes launched during the March 1999 experiment. As

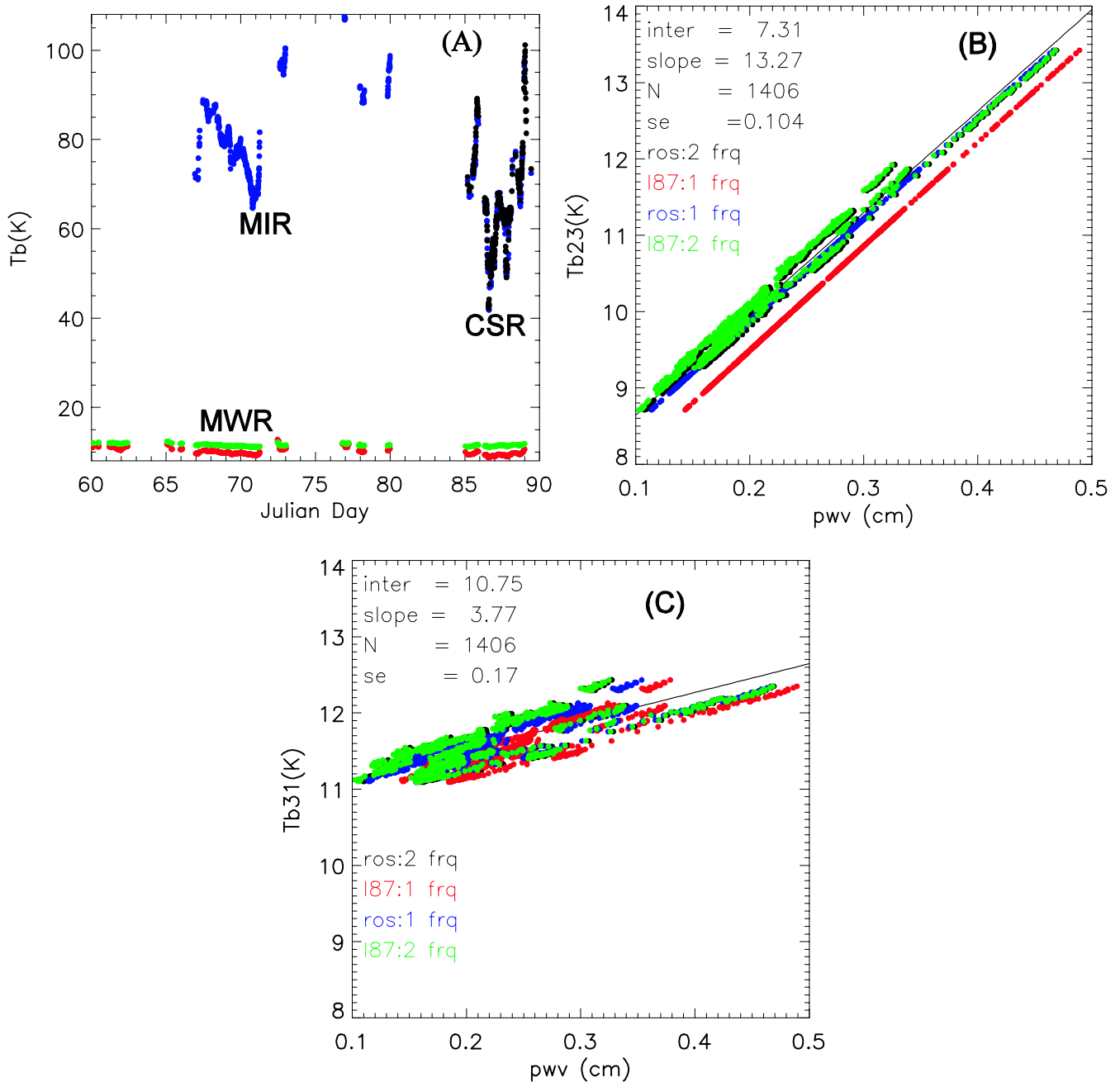


Figure 1. T_b for ARM MWR, the ETL CSR (183 +/- 7 GHz), and the NASA MIR (183 +/- 7 GHz). (A) Time series of T_b 's measured during clear conditions. (B) T_b at 23.8 GHz vs. PWV inferred from retrievals from 2-freq MWR data based on ROS absorption model. (C) T_b at 31.4 GHz vs. PWV inferred from retrievals from 2-freq MWR data based on ROS absorption model. In (B) and (C) the corresponding two-frequency retrievals from L87 as well as the single-frequency retrievals from L87 and ROS are shown.

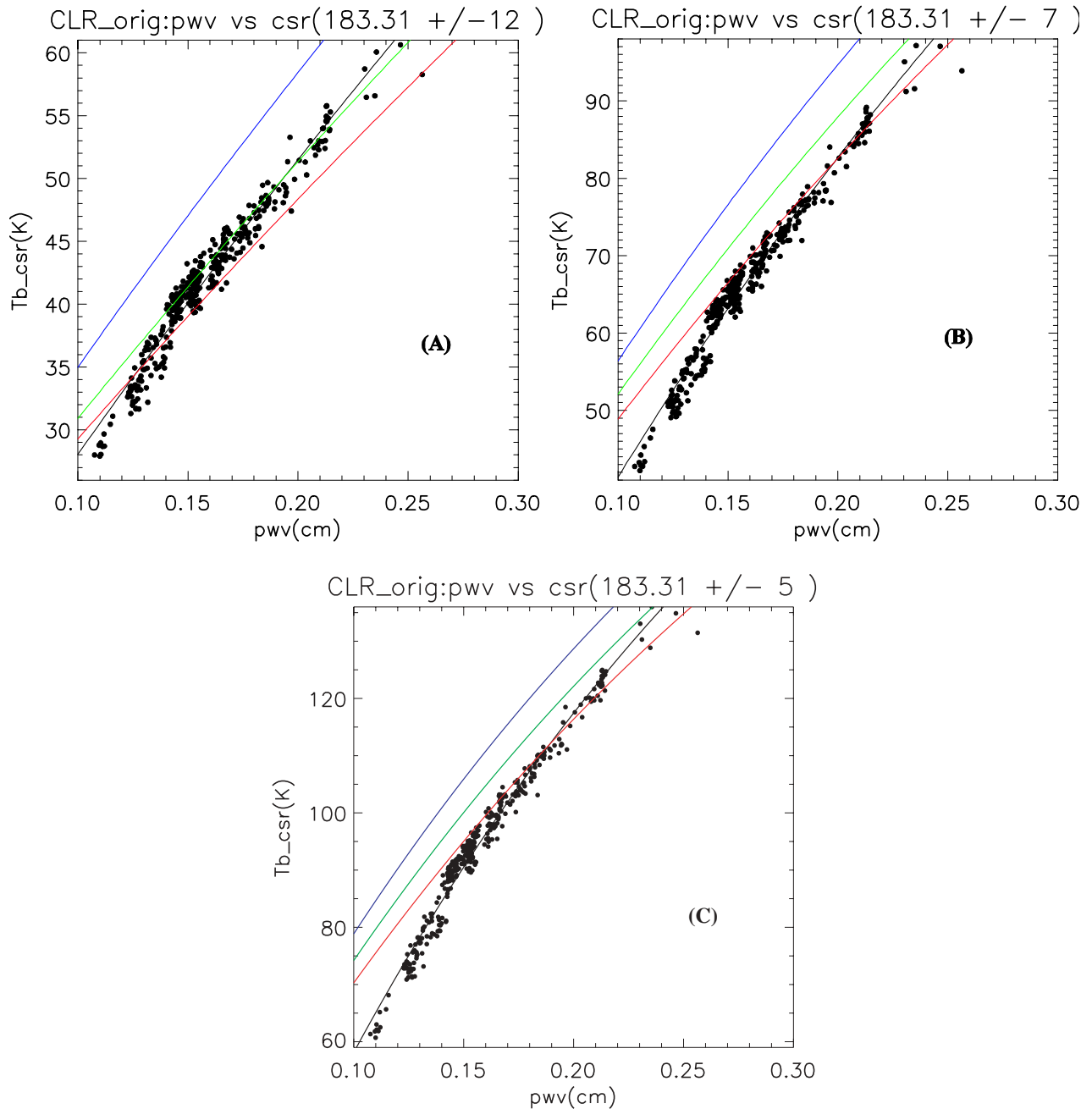


Figure 2. Comparisons of CSR-measured T_b vs. PWV measured by the ARM MWR during clear (CLR) conditions. The black curve is a nonlinear fit to the measured data; blue corresponds to L93; green to L87, and red to ROS. The nonlinear fit was based on Equations (1) and (2) using the parameters τ_d and κ . (A)- 183.31 ± 12 ; (B)- 183.31 ± 7 ; (C)- 183.31 ± 5 GHz.

has been observed consistently from a variety of data, L93 overestimates T_b . It is also apparent, that neither L87 nor ROS completely agree with the measurements. At the lowest amounts of PWV, below 1.5 mm, the CSR measurements are consistently lower than that calculated from the models; this could

be an artifact due to the low sensitivity of the MWR to PWV, or to temperature dependences of line strengths and widths near 183 GHz. We plan to investigate this further.

MIR- and CSR- T_b vs. MWR-PWV

In addition to measurements made near the 183 GHz absorption line, MIR observations were made at 150 and 220 GHz (see Figure 3). In Figure 4, we also show CSR and MIR observations at 183 ± 7 and 340 GHz. It is especially encouraging that there is excellent agreement between instruments at these frequencies.

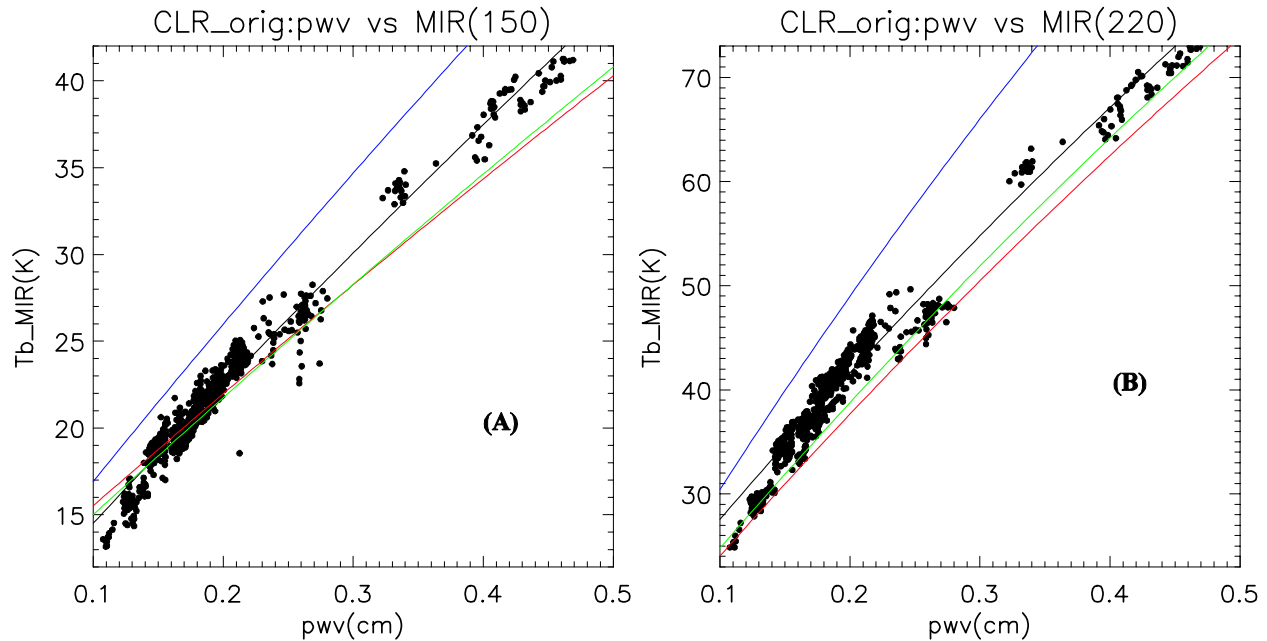


Figure 3. Measured MIR- T_b vs. PWV retrieved from the ARM MWR. The colored lines follow the same notation as in Figure 2. (A)-150; (B)-220 GHz.

Comparison of T_b from the MWR and MIR with Radiosonde-Based Calculations

Radiosonde observations were taken once a day at the CART site using Vaisala RS80H radiosondes, and twice daily by the National Weather Service, roughly 5 km from the radiometers. Because of humidity problems known to be associated with the RS80H radiosondes, a Vaisala correction algorithm was applied to these data. Cloud screening was implemented by the use of the Vaisala 25K cloud ceilometer and we used only radiometric data that were determined to be clear ± 30 min from the radiosonde release time. The results of comparisons using L87, L93, and ROS are shown in Table 1.

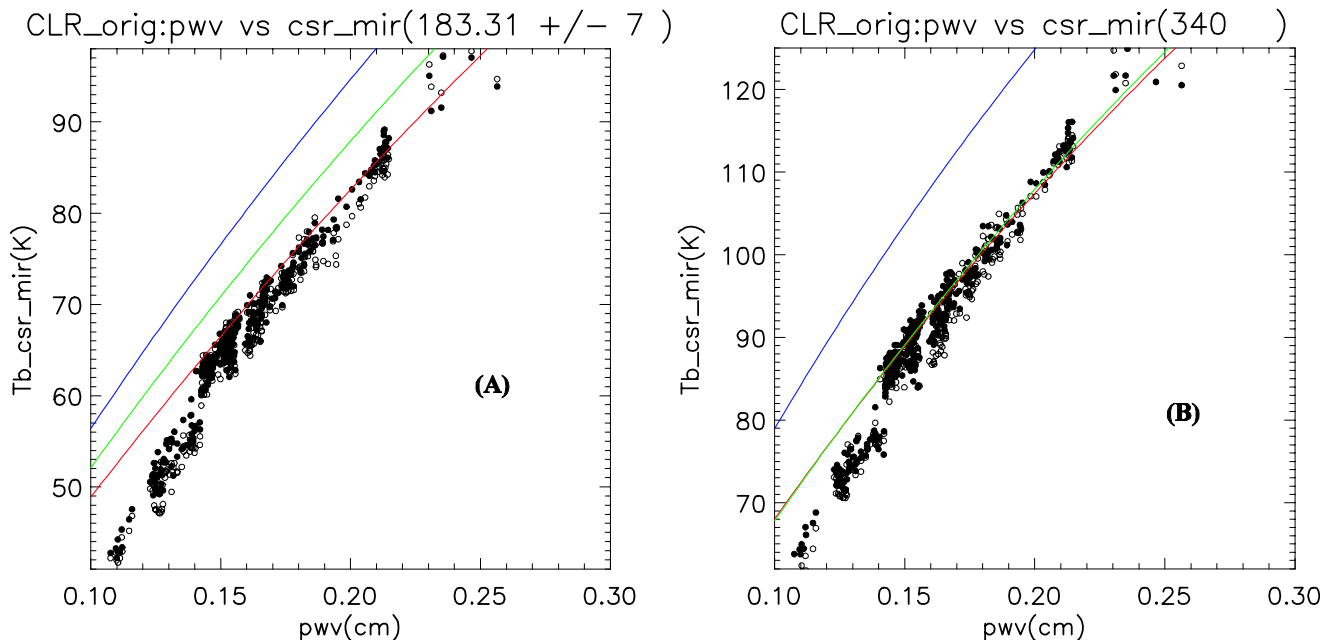


Figure 4. Measured and calculated (colored) T_b vs. PWV for CSR (open circles) and MIR (full circles). Both the CSR and the MIR were independently calibrated yet demonstrate excellent agreement. The colored lines follow the same notation as in Figure 2. (A)- 183.31 ± 7 , (B) 340 GHz.

Conclusions

We have presented a variety of measured and calculated data to show the potential of millimeter wavelength radiometric measurements to measure water vapor during arctic conditions. We have focused on the more transparent channels because completely independent calibration methods were used for these data. The MIR calibrations relied entirely on black body reference target measurements while CSR used the tipcal method. For the frequencies in common, the agreement in measured T_b was excellent, of the order of 1 to 2 K. However, there are major uncertainties in the forward model calculations revealed by the March 1999 experiment. For the MWR channels, the L93 model agreed best with the measurements with a 0.11 K bias and a standard deviation of 0.19 K rms. However for the millimeter-wave channels, the L93 model significantly over predicted TB. It is clear that the L93 model does not satisfactorily represent the submillimeter wavelength data and differs substantially from either L87 or ROS. However, at some, but not all, frequencies there is significant difference between L87 and ROS. The uncertainties in RAOB measurements of water vapor, coupled with MIR and CSR calibration uncertainties of ~ 3 K, did not allow us to make a clear choice between the L87 and ROS absorption models. The observed differences could be due to uncertainty in radiosonde data, absorption models, radiometer calibration, and small sample size, or, most likely a combination of all four. It is clear that these difficulties, important not only to ARM water vapor studies but also to the remote sensing community at large, will be overcome only if a much larger sample size of coincident radiosonde and radiometer data is available. ETL plans to repeat the 1999 experiment in February-March of 2004, with particular emphasis on more frequent and mixed types of radiosondes, and improved radiometric calibrations. Zenith brightness temperatures collected during the intensive observation period along with data documentation are available on the ARM archive (www.arm.gov).

Table 1. Average and standard deviation of (Measured – Calculated) TB(K) for three absorption Models. Clear conditions determined from ceilometer. Measured data are 1-hr averages centered around NWS and ARM radiosonde release times. Sample sizes: NWS = 18 and ARM_COR = 9. The average PWV for NWS and ARM radiosondes was 0.208 and 0.201 cm, respectively.

MWR 23.8	L87-AVG	L87-SDE	ROS-AVG	ROS-SDE	L93-AVG	L93-SDE
NWS	0.55	0.19	0.17	0.19	-0.11	0.19
V_COR	0.55	0.40	0.18	0.37	-0.11	0.37
MWR 31.4						
NWS	0.82	0.09	0.28	0.09	-0.01	0.09
V_COR	0.81	0.11	0.27	0.10	-0.03	0.10
MIR 90						
NWS	-1.03	0.31	-1.72	0.32	-0.51	0.32
V_COR	-0.98	0.52	-1.65	0.45	-0.48	0.45
MIR 150						
NWS	0.65	1.55	0.31	1.69	-3.52	1.69
V_COR	0.54	1.25	0.24	1.15	-3.67	1.15
MIR 220						
NWS	-3.62	4.68	1.24	4.79	-10.14	4.79
V_COR	-4.54	6.08	0.30	5.17	-10.90	5.17
MIR 340						
NWS	0.41	5.65	0.69	5.70	-15.86	5.70
V_COR	0.72	5.65	1.00	5.23	-14.99	5.23
MIR 183+/-7						
NWS	3.14	2.57	4.15	2.58	-6.82	2.58
ARM_COR	2.46	2.98	3.50	2.66	-7.50	2.66

Acknowledgement

The work presented in this paper was sponsored by the Environmental Sciences Division of the U.S. Department of Energy as a part of their Atmospheric Radiation Measurement Program.

Corresponding Author

E. R. Westwater, Ed.R.Westwater@noaa.gov, (303) 497-6527

References

Han, Y., and E. R. Westwater, 2000: Analysis and improvement of tipping calibration for ground-based microwave radiometers. *IEEE Trans. Geosci. Remote Sens.*, **38**, 1260-1277.

Han, Y., E. R. Westwater, P. E. Racette, W. Manning, A. Gasiewski, and M. Klein, 2000: Radiometric observations of water vapor during the 1999 Arctic Winter Experiment. In *Proceedings of the Tenth Atmospheric Radiation Measurement (ARM) Science Team Meeting*, U.S. Department of Energy, Washington, D.C. Available URL: http://www.arm.gov/docs/documents/technical/conf_0003/han-y.pdf

Liebe, H. J., and D. H. Layton, 1987: *Millimeter wave properties of the atmosphere: Laboratory Studies and Propagation Modeling*. National Telecommunications and Information Administration (NTIA) Report 87-24, p. 74.

Liebe, H. J., G. A. Hufford, and M. G. Cotton, 1993: "Propagation modeling of moist air and suspended water/ice particles at frequencies below 1000." AGARD Conf. Proc. 542, Atmospheric propagation effects through natural and man-made obscurants for visible through MM-wave radiation, pp. 3.1-3.10. (Available from NASA Center for Aerospace Information, Linthicum Heights, Maryland).

Liljegren, J. C., 2000: "Automatic self-calibration of ARM microwave radiometers." In *Microwave Radiometry and Remote Sensing of the Earth's Surface and Atmosphere*, P. Pampaloni and S. Paloscia, Eds. VSP Press, pp. 433-441.

Racette, P., E. Westwater, Y. Han, W. Manning, A. Gasiewski, and D. Jones, 2000: "Millimeter-wave measurements of low amounts of precipitable water vapor," Proc. IGARSS'2000, July 24-28, 2000, pp. 1154-1156.

Rosenkranz, P. W., 1998: Water vapor microwave continuum absorption: a comparison of measurements and models. *Radio Sci.*, **33**, 919-928.